Dissociated jerk-limited trajectory applied to time-varying vibration reduction

Richard Béarée*, Adel Olabi

Arts et Metiers ParisTech, CNRS (UMR 7296), LSIS 8, Bd Louis XIV, 59046 Lille, France

ABSTRACT

Jerk-limited trajectories are a widespread solution for the trajectory planning of industrial machines-tools or robots. It is known that jerk limitation can reduce vibrations and in some cases can totally suppress residual vibration induced by a lightly damped stationary mode. However, for systems with time-varying mode, which is classically the case for configuration dependent mode or load mass variations, the previous result vanishes. This paper proposes to extend the jerk-limited profile (JL) properties to time-varying vibration problem. First, a guideline for designing a dissociated jerk-limited profile (DJL) based on simple and pragmatic Finite Impulse Response (FIR) filtering methodology is presented. Following the guideline, the time-varying vibration reduction principle is detailed. Then, experiments conducted on an industrial 3-axes Cartesian manipulator are presented. The experimental results show that the residual vibration magnitude is reduced to less than 23% of the original level obtained with JL profile and the settling time is reduced by 10%, demonstrating the efficiency of the proposed DJL trajectory planning.

1. Introduction

Vibration-free positioning is a basic objective in trajectory planning problem for a large class of industrial machines (manipulator, machine-tool or robot). Trajectory with infinite jerk (slope of acceleration) presents discontinuities that regulators cannot follow, whatever the performances of the actuators. These discontinuities excite the structure in transitory stages and are mainly responsible for mechanical deformations and vibrations. The use of a bounded jerk value (time derivative of acceleration) is known to limit the oscillatory behavior, hence the residual vibrations at the end of the motion. Numerous works, mainly within the framework of robotics but also in the machine-tool field, deal with the optimization of jerk-controlled trajectory [1,2], and in particular deal with the realization of minimum-jerk trajectory [3,4], minimum-time jerk trajectory [5] and continuity of jerk using spline interpolation methods or harmonic functions [6–8]. Trajectory based on minimization of jerk reduces mechanical stresses and vibrations because of their similarity with the motion of human arm [9]. When experimentally tested, such trajectory gives good overall results along the specified path, without any a priori knowledge of the vibratory behavior of the system. The corollary is that such profile cannot totally suppress residual vibrations. On the opposite, input shaping technique focus specifically on the cancellation of residual vibrations [10,11]. The method is based on the convolution of impulses with a minimum-time acceleration limited trajectory. According to the complexity of the filter used (called "shaper"), the robustness can be adapted to the behavior of the system. For instance, works presented in [12] demonstrate the effectiveness of shaping method on an industrial 6 axis robot.

Jerk-limited trajectory (JL), which is of interest in this paper, are available in modern CNC controller and can be seen as a "hybrid" solution between optimized-jerk trajectory and zero-vibration shaped trajectory. In [13,14] authors experimentally demonstrate that for a JL profile, the maximum jerk value, or is corollary the jerk time, can be specified to significantly reduce residual vibrations magnitude for system submitted to a lightly damped stationary mode. Now, considering systems with time-varying mode, which is classically the case for configuration dependent mode or load mass variations, the robustness of the JL profile is not sufficient to ensure vibration-free positioning. This paper proposes to extend the jerk-limited profile (JL) properties to time-varying vibration problem.

The paper is organized as follow: First, a guideline for designing JL profile and dissociated jerk-limited profile (DJL) based on simple and pragmatic FIR filtering methodology is detailed in Section 2. In Section 3, the vibration cancellation method is explained and the time-varying vibration reduction principle is presented. Experiments conducted on an industrial 3-axes Cartesian manipulator are presented and analyzed in Section 4.
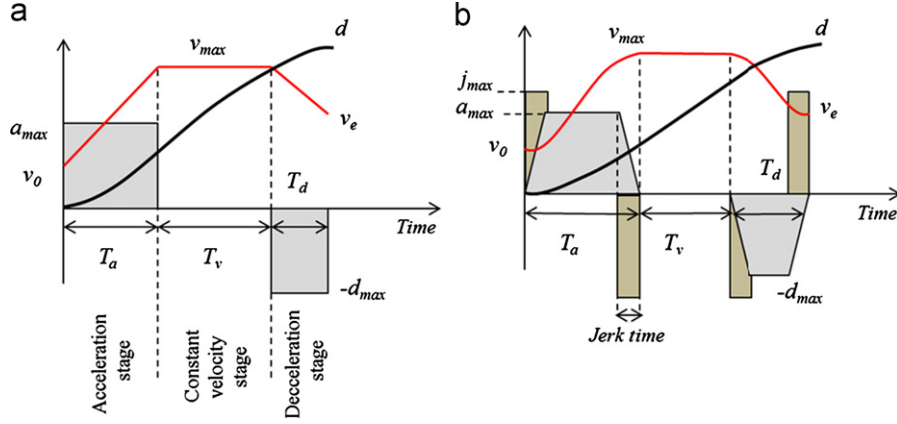
Fig. 1. Acceleration-limited (a) and jerk-limited (b) profiles.

2. Dissociated jerk-limited profiles synthesis

A simple method to plan a motion with specified maximum acceleration and velocity consists of using an acceleration-limited trajectory (sometimes called acceleration bang-bang or trapezoidal velocity profile). Fig. 1 presents such profile, which can be divided into three stages. In the first stage, with time period T_a, the acceleration is constant and the velocity is a linear function of time starting from the initial value v_0 to the final value v_{max}. In the second stage the acceleration is null and the velocity is constant during a period noted T_v. For the last stage, the acceleration is negative (assuming a positive displacement) and the velocity decreases linearly during T_d with v_e representing the ending velocity. Typically, the maximum acceleration and deceleration values (noted a_{max} and d_{max} in Fig. 1) are the same.

Assuming that the specified displacement d allows reaching the maximum velocity, calculating the area under the acceleration profile, the relations between maximum velocity, acceleration and stage time T_a and T_d will be given by

$$a_{max}T_a = v_{max} - v_0; \quad a_{max}T_d = v_{max} - v_e \tag{1}$$

The travel length generated during these acceleration/deceleration stages is the minimum distance, noted d_{min}, for which the maximum velocity is reached. Integrating the velocity profile during these two stages gives:

$$d_{min} = \frac{T_a(v_{max}-v_0)}{2} + T_a v_0 + \frac{T_d(v_{max}-v_e)}{2} + T_d v_e$$
$$d_{min} = \frac{(2v_{max}^2 - v_0^2 - v_e^2)}{2a_{max}} \tag{2}$$

The constant velocity stage time is then given by the remaining distance to be traveled:

$$T_v = \frac{d - d_{min}}{v_{max}} \tag{3}$$

Considering now the case where d is lower than d_{min}, the velocity profile is triangular and the reachable velocity has to be recalculated by replacing d_{min} by d in (2). The new v_{max} can then be inserted in (1) to calculate the acceleration/deceleration stages. Hence, acceleration-limited profile can be easily planned using the following algorithm[1] (given in continuous time domain form):

if $d \geq d_{min}$

---

then $T_a = \dfrac{v_{max} - v_0}{a_{max}}; \quad T_d = \dfrac{v_{max} - v_e}{a_{max}}; \quad T_v = \dfrac{d - d_{min}}{v_{max}}$

else $T_v = 0; \quad T_a = \dfrac{1}{2a_{max}}\left((v_0 - v_e) + \sqrt{4da_{max} - (v_0 - v_e)^2}\right);$

$$T_d = \frac{1}{2a_{max}}\left((v_e - v_0) + \sqrt{4da_{max} - (v_0 - v_e)^2}\right) \tag{4}$$

Modern controllers use smoother profiles to obtain more continuous velocity by classically adding a constraint on the jerk. The resulting profile is a jerk-limited (JL) profile or S-curve velocity profile, presented in Fig. 1, and is then composed of seven stages (each previous acceleration or deceleration stages can be divided into three stages). JL trajectory can be analytically described but at the expense of a more complex algorithm [15]. The method used in this paper takes advantage of the property of finite impulse response filter (FIR) to easily obtain a JL profile based on a simple acceleration limited profile described by (4). This solution has two main advantages: Easiness of implementation as compared to analytically defined jerk profile and real-time adaptation for existing controller (less computer time consuming).

2.1. FIR filtering method

A ramp profile can be basically obtained by filtering a step function, note $e(t)$ with a continuous filter $f(t)$ described by the transfer function

$$F(s) = \frac{1}{T_F}\left(\frac{1 - e^{-T_F s}}{s}\right) \tag{5}$$

where T_F is the filter time and s the Laplace operator. The convolution of the step function of amplitude E with $f(t)$ corresponds to the product of the Laplace transforms of each function

$$L[e(t)*f(t)] = E(s)F(s) = \frac{E/T_F}{s^2}(1 - e^{-T_F s}) \tag{6}$$

Fig. 2 shows the ramp profile resulting from (6).

Noting T_e the sampling time of the signal and using the backward difference method, the z-transform of the FIR filter equivalent to (5) will be given by

$$F(z) = \frac{1}{N_F}\left(\frac{1 - z^{-N_F}}{1 - z^{-1}}\right) \tag{7}$$

with N_F, the round integer of T_F/T_e. This FIR filter is equivalent to a moving averaging filter and noting respectively F_k and I_k the output and input value of the filter at time kT_e, it can be more

---

[1] This algorithm supposes that the commanded displacement is feasible, i.e. that the extremum velocities values are chosen compatible with the specified displacement. Classically, the controller look-ahead function pre-analyses the trajectory and fixed the initial and final velocity values before any motion.

naturally defined for implementation as

$$F_k = \frac{1}{N_F} \sum_{i=1}^{N_F} I_{k-i+1} \tag{8}$$

Thus, a JL profile with specified maximum jerk value, noted j_{max}, can be obtained by convolving the previous FIR filter with a limited-acceleration profile, such as the one depicted in Fig. 1. Next section describes the adaptation of the initial acceleration-limited profile to prepare it for the filter convolution, i.e. to take account of the filter time effect.

2.2. Adaptation of the acceleration-limited profile for FIR filtering

The filter time will theoretically be fixed by the relation $T_F = a_{max}/j_{max}$. One notes that for implementation, T_F will be near the closest multiple of the sampling time T_e. To take account of filter time effect, some adaptations of the initial acceleration-limited profile have to be done before applying the filter. For clarity reasons, Fig. 3 presents these adaptations on the velocity profile only:

1) First, with respect to the ending velocity (even if null) after the filter convolution, a constant ending velocity stage of time length equal to the filter time T_F is added (the final velocity value is maintained during N_F sampling time).
2) Second, with respect to the specified displacement d, its value has to be initially modified when we calculate the acceleration-limited profile as follows:

$$d = d - \Delta d \tag{9}$$

with Δd the additional displacement induced by this ending constant velocity stage. This extra displacement at constant velocity v_e can be calculated, after convolution with (8) as

$$\Delta d = \frac{1}{N_F} \sum_{i=1}^{N_F} v_e T_e i = v_e T_e \frac{(N_F + 1)}{2} \tag{10}$$

3) Finally, with respect to the constraint on the maximum jerk value for displacement with no constant velocity stage, the time T_v has to be low-bounded by T_F and then v_{max} has to be recalculated. This case is depicted in Fig. 3(b).
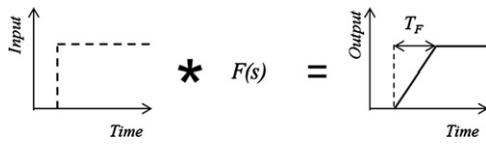

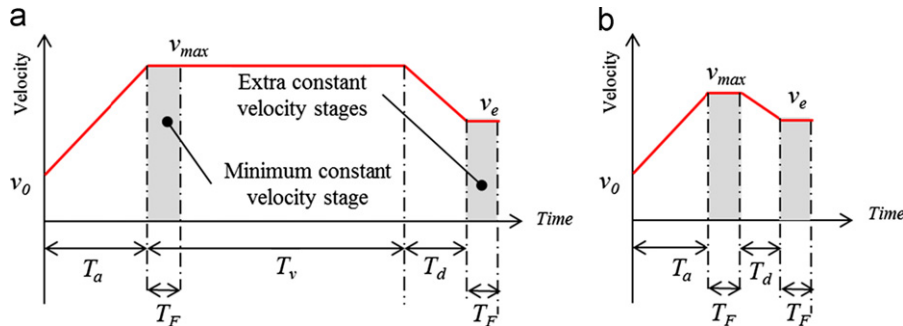**Fig. 2.** Filtering of a step function with $F(s)$.

The algorithm corresponding to the adapted limited-acceleration profile, taking account of the sampling time T_e, is detailed in the appendix. Fig. 4 shows a jerk-limited profile resulting from the FIR filtering method applied to the preceding adapted profile. Motion time, T_F, is increased compared to classical acceleration-limited profile. Fig. 5 presents an application of the proposed methodology to a multi-segment motion. This profile can be used as curvilinear abscissa motion law on a specified parametric geometry for end-point motion (tool, effector) of an industrial machine.

2.3. Dissociated jerk-limited profile (DJL)

As we will detail in the next section, the jerk time can be specified to significantly reduce residual vibrations magnitude for system submitted to a lightly damped stationary mode. This paper proposes to extend the jerk-limited profile (JL) properties to time-varying vibration problem by using a jerk-limited profile with different maximum jerk values (i.e. different jerk times). Keeping the previous methodology based on FIR filtering and using the distributivity property of convolution, a simple solution consists of splitting the previously seen adapted acceleration-limited profile into four parts (four acceleration step functions), as depicted in Fig. 6. Fig. 7 shows an illustration of the methodology used for the synthesis of DJL profile. The acceleration a_{DJL} corresponding to the DJL profile results from a simple combination of the four steps of the adapted acceleration profile, each step being filtered with a different buffer length. According to Fig. 7 notations, the position d_{DJL} of DJL profile will be expressed as

$$d_{DJL}(s) = \frac{1}{s^2} \sum_{i=1}^{4} \frac{a_i}{s} F_i(s) e^{-T_i s}, \tag{11}$$

with $a_i = [a_{max} - a_{max} - d_{max} d_{max}]$, T_i the ith commutation times and F_i the ith FIR filters.

As previously seen, the adapted acceleration profile of Fig. 6 can be easily calculated (see Appendix). Here, the imposed parameters are the minimum constant velocity stage T_F before filtering and the extra constant velocity stage T_{MF} (see Fig. 6). Compared to acceleration-limited profile, the motion time of DJL profile, T_{MF}, is increased which is the mean value of the four filters times

$$T_{MF} = \sum_{i=1}^{4} T_{Fi}/4 \tag{12}$$

with T_{Fi} ($i = 1, 2, 3, 4$) the expected jerk times for the four stages. Time T_F ensures with respect to the jerk times for motion with no constant velocity. This stage length is simply the mean value of the two middle filter times

$$T_F = \frac{T_{F2} + T_{F3}}{2} \tag{13}$$

Fig. 3. Adaptations of the initial acceleration-limited profile for FIR filtering (*case a*: v_{max} is reach, *case b*: v_{max} is reduced).
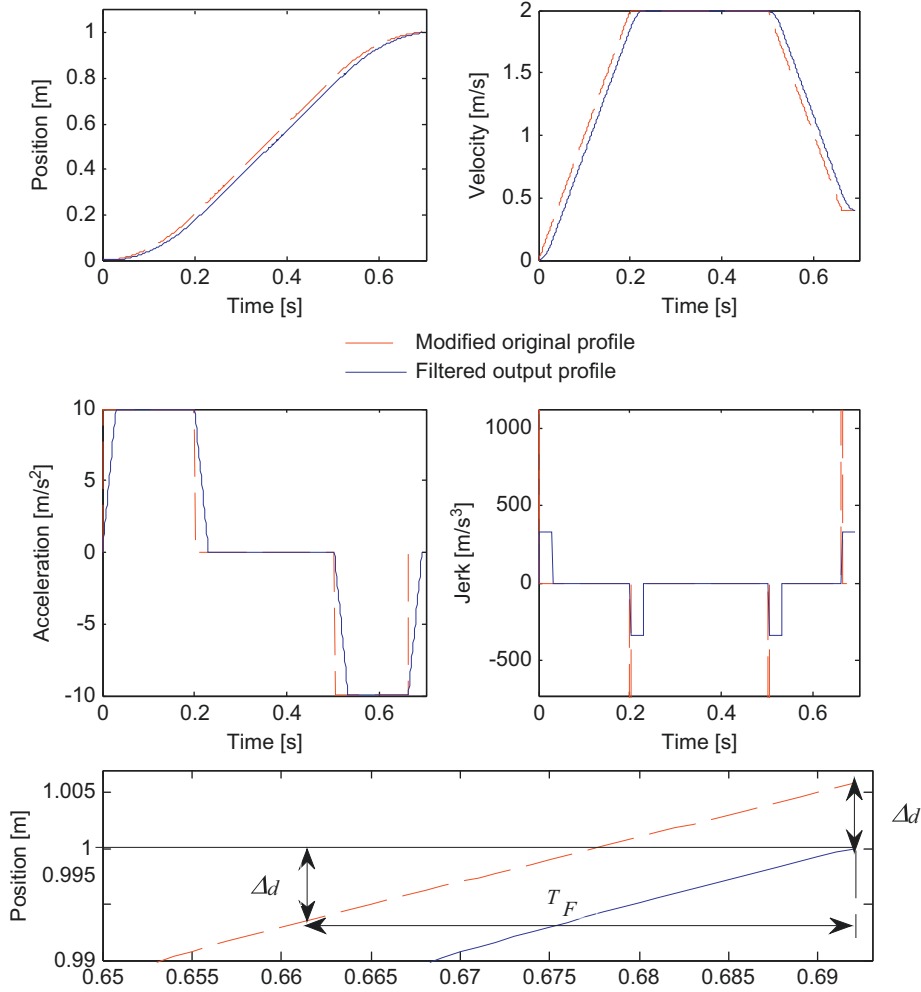
Fig. 4. Adapted acceleration-limited profile and resulting JL profile after filtering ($T_e=1$ ms, $T_F=30$ ms, $a_{max}=10$ m/s², $v_{max}=2$ m/s, $v_e=0.4$ m/s, $d=1$ m).

Then, the next step consists of calculating the commutation times T_i according to the predetermined parameters of the initial profile T_a, T_v, T_d and according to the expected jerk times T_{Fi} for each stages. Considering initial velocity as null and T_1 equal to T_a, then the maximum velocity reach after acceleration stage for DJL profile can be expressed in continuous time domain as

$$\max(v_{DJL}) = \lim_{s \to 0} s \frac{a_{max}}{s^2}(F_1(s) - e^{-T_a s}F_2(s))$$
$$= \lim_{s \to 0} s \frac{a_{max}}{s^2}\left(\frac{(1-e^{-T_{F1}s})}{s} - e^{-T_a s}\frac{(1-e^{-T_{F2}s})}{s}\right)$$
$$= T_a a_{max} + \frac{T_{F2} - T_{F1}}{2}$$
$$= v_{max} + \frac{T_{F2} - T_{F1}}{2} \tag{14}$$

Thus, with respect to the maximum (or reachable) velocity, the step time T_1 has to be taken as

$$T_1 = T_a - \frac{T_{F2} - T_{F1}}{2} \tag{15}$$

In the same way, times T_2 and T_3 are given by

$$T_2 = T_1 + T_v - T_F$$
$$T_3 = T_2 - \frac{T_{F4} - T_{F3}}{2} \tag{16}$$

One notes that for implementation aspect, the jerk times have to be rounded in such manner that the times given by (15) and (16) are multiple integers of the sampling time. Now, if T_1 or T_3 has a negative value (T_2 cannot be negative because by construction T_v is low-bounded by T_F), then the considered stage is too short to use the proposed methodology. However, in this case there no real interest to dissociate the jerk times and it seems better to use a jerk-limited profile for acceleration and/or deceleration stages ($T_{F2}=T_{F1}$ and/or $T_{F4}=T_{F3}$). Fig. 8 shows the flowchart of the proposed method for DJL profile synthesis. Figs. 9 and 10 present two representative examples of DJL, which demonstrate that this filtering methodology can be efficiently used for DJL trajectory planning.

3. Adaptation to the vibratory behavior of the system

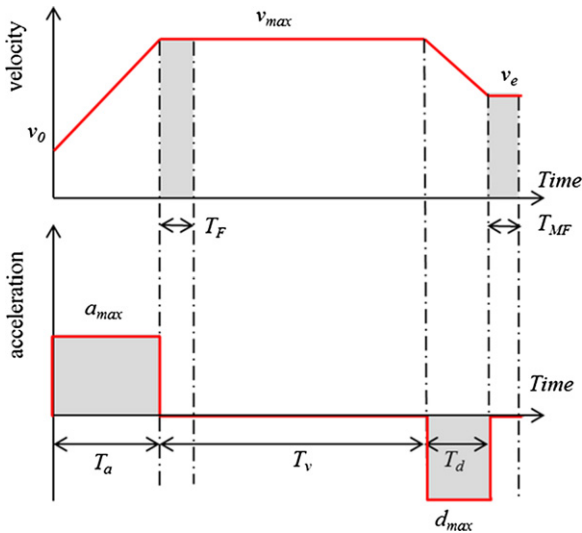### 3.1. Jerk time influence on vibratory phenomena

Maximum jerk value for industrial machines is classically tuned empirically or experimentally based on satisfactory behavior of the system during the motion. It is known that compared to acceleration-limited profile, jerk-limited profile can reduce vibrations and in some cases can totally suppress residual vibration [13]. Such a profile can be seen as a sum of time delayed impulses convolved with a jerk step. In continuous time domain, the position resulting from a jerk-limited profile can be written as

$$d_{JL}(s) = \frac{j_{max}}{s^4} \sum_{i=1}^{n} A_i e^{-sT_i} \tag{17}$$

with n the number of commutation ($n=4$, 6 or 8 according to dynamic limitations). The coefficients A_i take their values in the ensemble $\{1, 2, -2, -1\}$ and T_i the switching times.
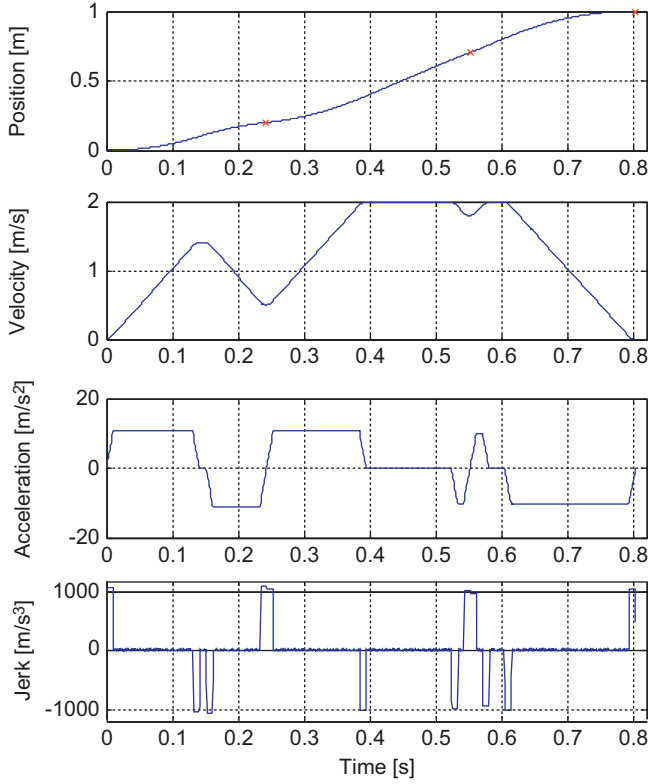
Fig. 5. JL trajectory resulting from FIR filtering method applied to a multi-segments motion ($T_e = 1$ ms, $T_F = 10$ ms, $d = [0, 20, 50, 3]$ m, $v_e = [0, 51, 80]$ m/s, $a_{max} = 10$ m/s^2, $v_{max} = 2$ m/s).

The impact of such a profile on vibration of a system can be easily calculated using the expression for residual vibration of a second-order harmonic oscillator of frequency ω rad/s and damping ratio ζ, which is given in [16]. The vibration from a series of impulses is divided by the vibration from a single unity-magnitude impulse to get the percentage of vibration:

$$Vib(\omega) = e^{-\zeta\omega T_n} \sqrt{\left(\sum_{i=1}^{n} A_i e^{\zeta\omega T_i} \cos(\omega_d T_i)\right)^2 + \left(\sum_{i=1}^{n} A_i e^{\zeta\omega T_i} \sin(\omega_d T_i)\right)^2},$$

(18)

with $T_n = \sum_{i=1}^{n} T_i$ and $\omega_d = \omega\sqrt{1-\zeta^2}$ the damped frequency.

Without loss of generality, considering the residual vibration for one stage of constant jerk (for example the first stage) and noting T_F the jerk time, the maximum jerk value is given by
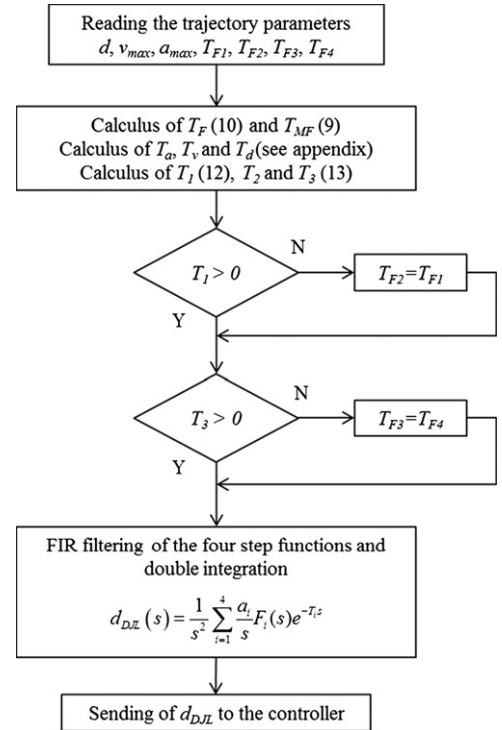
$$j_{max} = a_{max}/T_F$$

(19)

and the percentage of vibration can be expressed as

$$Vib(\omega) = \frac{a_{max}}{T_F} e^{-\zeta\omega T_F} \sqrt{1 + e^{2\zeta\omega T_F} - 2e^{\zeta\omega T_F}\cos(\omega_d T_F)}$$

(20)

Assuming a lightly damped mode ($\zeta = 0$), Eq. (9) is rewritten as

$$Vib(\omega) = \frac{2a_{max}}{T_F} \sin\left(\frac{\omega T_F}{2}\right) = \omega a_{max} \frac{\sin(\omega T_F/2)}{\omega T_F/2}$$

(21)

Thus, residual vibration for undamped mode is a sine cardinal function of the jerk time T_F. The decreasing envelop is obviously linked to Eq. (19), which imposed to reduce the maximum jerk value (thus the excitation magnitude) according to the increase of jerk time. To cancel residual vibration after each sequence of two

Fig. 8. Flowchart of the proposed methodology for DJL profile synthesis.

Fig. 6. Parameterization of the adapted limited-acceleration profile.

Fig. 7. Illustration of DJL profile synthesis principle.
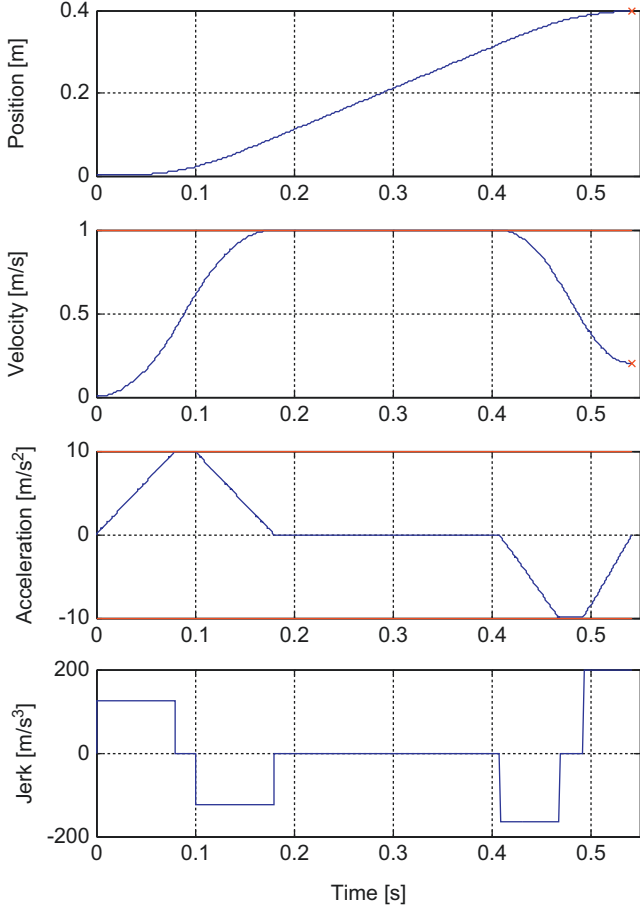
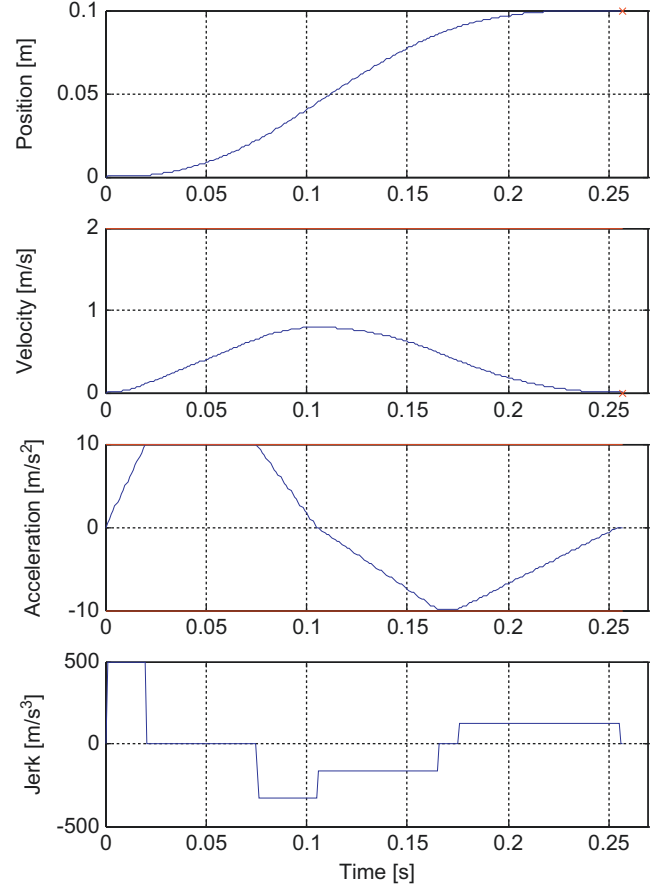**Fig. 9.** Example 1 of dissociated jerk profile resulting from the filtering strategy (T_e=1 ms, a_{max}=10 m/s², v_{max}=1 m/s, T_{F1}=T_{F2}=80 ms, T_{F3}=60 ms, T_{F4}=50 ms, v_e=0.2 m/s, d=0.4 m).


Fig. 10. Example 2 of dissociated jerk profile resulting from the filtering strategy (T_e=1 ms, a_{max}=10 m/s², v_{max}=1 m/s, T_{F1}=20 ms, T_{F2}=30 ms, T_{F3}=60 ms, T_{F4}=80 ms, v_e=0 m/s, d=0.1 m).

jerk commutations, a trivial solution consists of choosing the jerk time equal to a multiple of the natural period of the vibration mode. Pragmatically, to ensure a minimum loss of theoretical motion time (but possible reduction of the system settling time) the minimum time of the moving average filter used in the planning methodology has to be chosen equal to the dominating natural period of the system. Fig. 11 illustrates the residual vibration function $Vib(\omega)$ given by (21) according to the jerk time (filter time T_F) and the damping ratio. Full-scale corresponds to the reference maximum vibration for acceleration-limited profile. The reduction of maximum residual vibration for increasing jerk time is induced by the relative reduction of maximum jerk value given by (19). For lightly damped mode it is possible to cancel residual vibration, on the other hand as soon as the mismatch between filter time and natural period increases this result vanishes. In order to keep the residual vibration below 20%, the tuning error also has to be lower than 20%. Of course, it is possible to overestimate the natural period to guarantee a specified level of residual vibration, but with a detrimental effect on the motion time. At last, one notes that a damping value below 10% has poor effect on the residual vibration level, which justifies the classical assumption of lightly damped modes for dominating deformations of industrial machines.

3.2. Dealing with time-varying vibration

Considering a system submitted during its motion to a significant frequency shift of a dominating vibration mode, the previous tuning methodology based on the jerk time becomes inadequate to
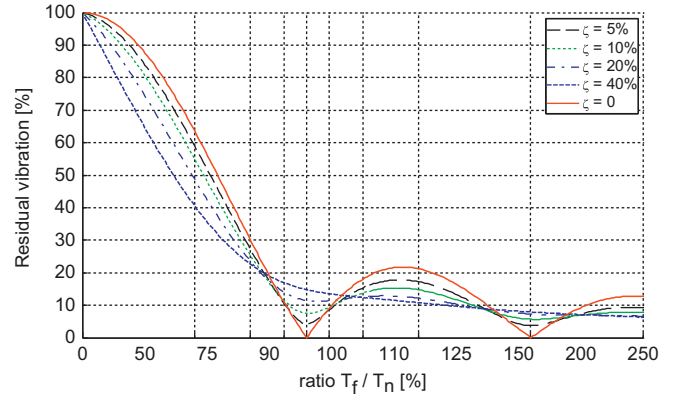
Fig. 11. Residual vibration according to the jerk time and damping ratio.

decrease substantially the vibrations. For industrial machines, this frequency shift is basically induced by the change of machine configuration during the motion and/or by load mass variations. The main idea developed in this paper consists of using a DLJ profile with potentially four different jerk times. Each constant jerk stage can be tuned to cancel the vibration mode at its time-dependent frequency value. The method is based on the main hypothesis that the variation of modal frequency during one constant jerk stage is negligible. Analytical expression of residual vibration, such as the relation (21), cannot be easily derived for a second order harmonic oscillator with time-varying frequency $\omega(t)$. Fig. 12 presents the simulated residual vibration after a constant jerk stage for linear and
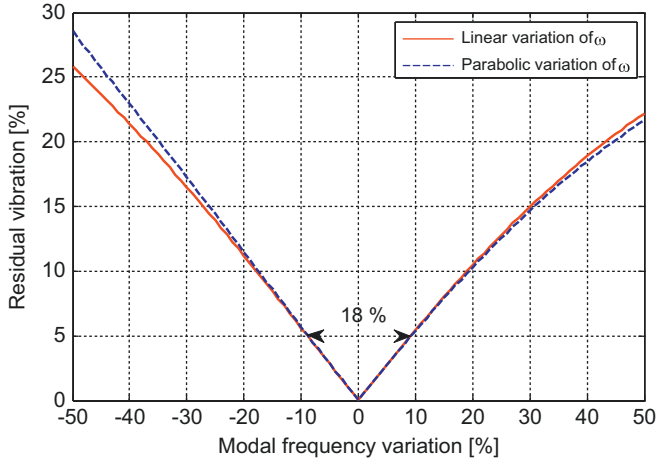
Fig. 12. Residual vibration at the end of a constant jerk stage according to the modal frequency time variation.

parabolic variation of frequency ω with time. Hence, residual vibration level would be kept below 5%, compared to acceleration-limited profile, if the variation of $\omega(t)$ is less than $\pm 9\%$ during one constant jerk stage. One notes that such a methodology cannot totally suppress residual vibration, but it can significantly improve the result obtained with current JL profile.

The proposed method supposes the knowledge of the modal frequency variation according to the spatial position of the system. The three following methods can be used:

- Lookup table coming from experimental cartography of the modal frequency within the system workspace.
- Real-time identification of the modal frequency based on sensor feedback.
- Analytical relation describing the variation.

The comparison of these methods is out of the scope of this study. In the following, the last one is used. The main reason is that for numerous mechanical systems, the dominating modal frequency shift can be approximated by simplified relation. For example, considering machines with Cartesian axes, the main source of modal parameter variation is a flexural deformation of one axis induced by the motion of another axis. Classically, the excited axis is the end-effector or load axis and can be assimilated to a cantilever beam submitted to bending moment. In this case, the corresponding modal period will theoretically evolve proportionally to the square of the axis length submitted to flexural excitation. But, according to the considered workspace, the variation can generally be linearized according to the axis position. Other class of systems is the study in [12], where authors verify the proportionality of the dominating modal period of a 6 axis industrial robot with a Cartesian position of the end-effector (deduced from the joints position). At last, considering load variations, which are encountered for pick and place operations, the modal period will evolve proportionally to the square root of the load mass. This last case does not imply continuous variation of the vibration along the motion, but punctual change of modal frequency according to the load. Thus, in this case a JL profile can be used with a jerk time tuned accordingly to the current load.

4. Experimental validations

In order to show the effectiveness of the control strategy adopted in the present work, experimental validations are carried out on a 3-axes Cartesian manipulator. Fig. 13 presents the
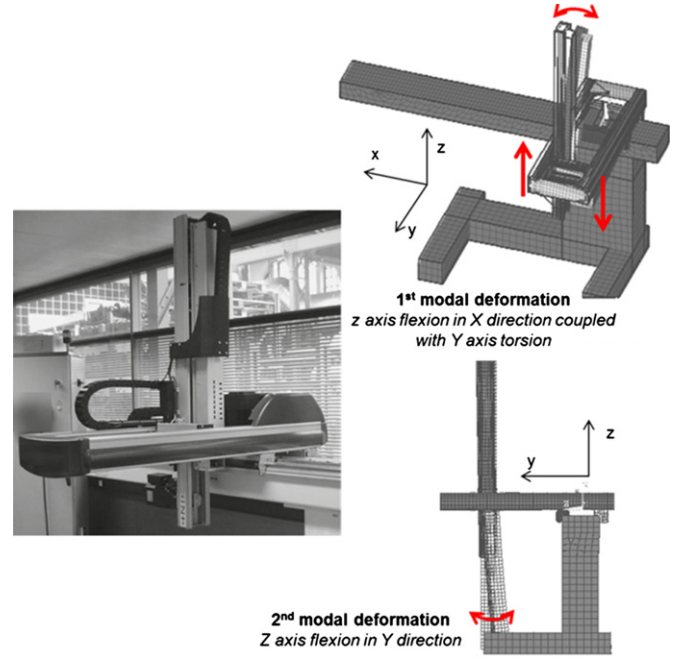
Fig. 13. Cartesian manipulator used for tests and dominating modal deformations in X and Y directions.
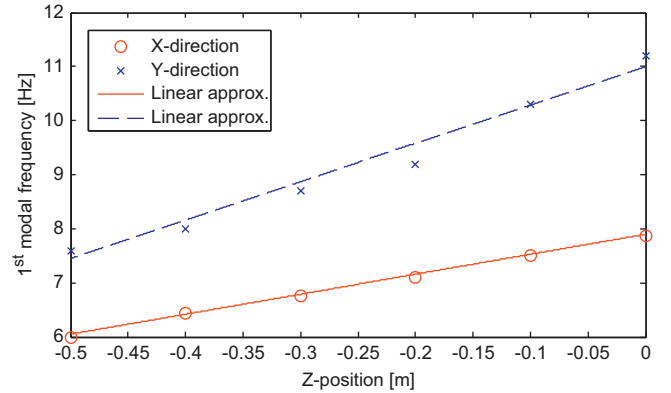
Fig. 14. Measurements of modal frequency variations in X and Y direction according to Z-axis position.

manipulator and its two dominating modal deformations, which are mainly induced by a flexural motion of the vertical Z-axis in X and Y directions. Hence, when the vertical Z-axis is moving, the two modal frequencies associated to the previous deformations evolve according to the Z-axis position. Experimental modal analysis by impact hammer was conducted to find the frequencies evolutions. The result is depicted in Fig. 14. The dominating frequencies evolutions in the range of measurements (500 mm) can be reasonably approximated as linearly dependent of the Z-axis position. Hence, for the considered range of Z-axis position, the first modal frequency can evolve of 25% in X direction and 33% in Y direction. It can be noticed that the measured damping ratio is lower than 8%, which implies that the manipulator can be considered as a low-damped system.

The studied DJL trajectory planning algorithm is implemented in a real-time control card (dSpace 1103), which is here used to send the references for each manipulator axis without any change of their control structure. The load response is measured by a laser tracker (API) with absolute accuracy of $\pm 10\,\mu m/m$ and a sampling frequency of 200 Hz. Experimental validations were

undertaken for X-axis or Y-axis motion, while Z-axis is moving as depicted in Fig. 15. For the tests, only the trajectory of the "excitation" axis (i.e. X or Y-axis) is of interest. One notes that the Z-axis trajectory is a classical JL motion, which is only synchronized with the other moving axes. Moreover, the JL trajectories used for comparison with DJL trajectories are always
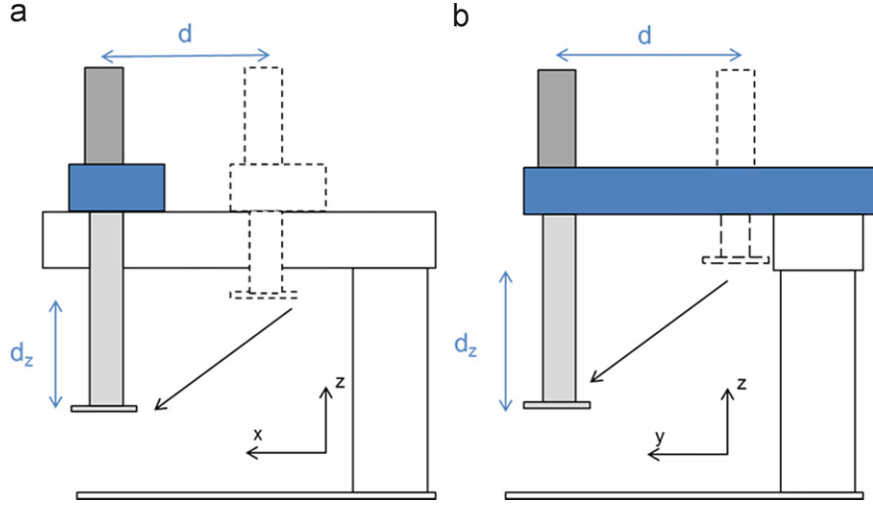
Fig. 15. Configurations of the tests (for the two configurations: $d=[0,10,20,30,40,5]$ m; $d_z=[0,10,20,30,40,5]$ m).
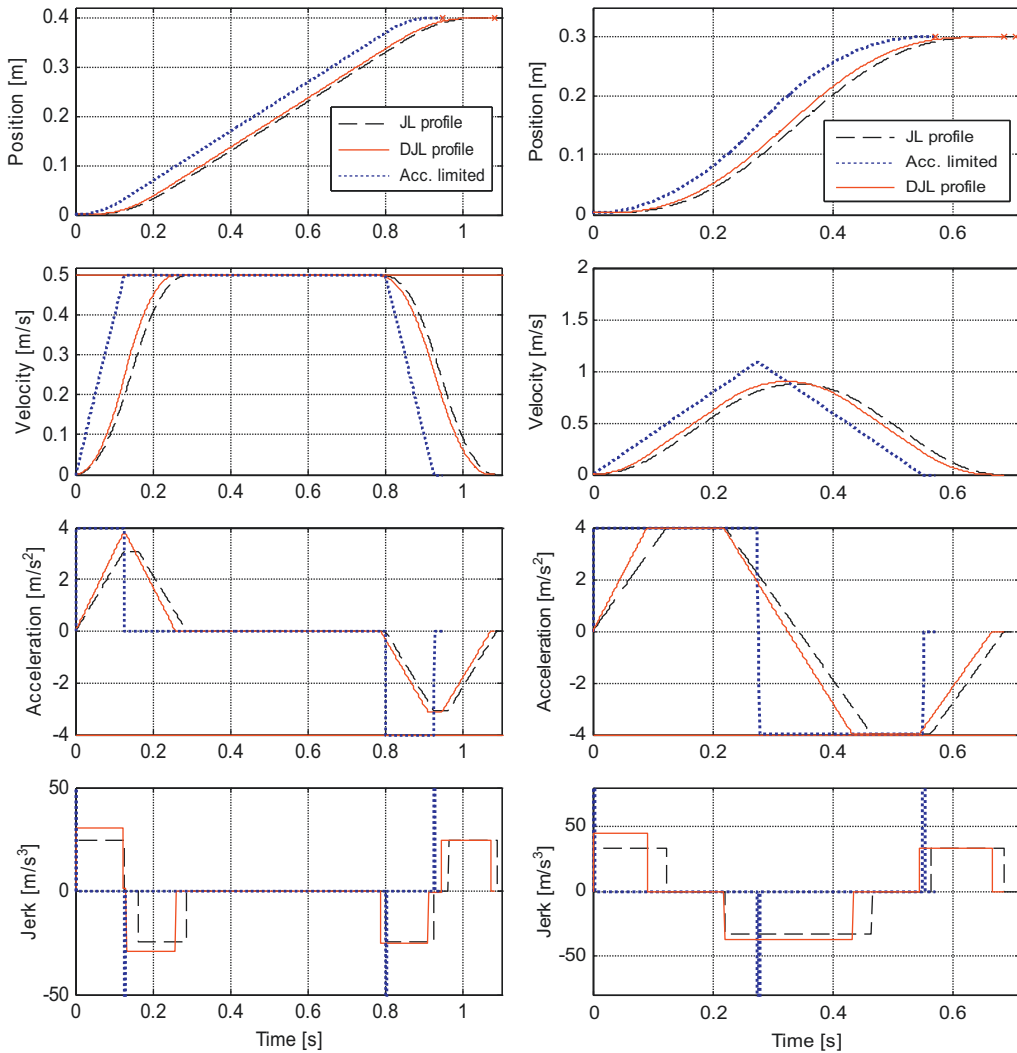
Fig. 16. Example of reference profiles for the tests: (left) motion in X-direction ($d=0.4$ m, $v_{max}=0.5$ m/s, $a_{max}=4$, $\Delta f=20\%$), (right) motion in Y-direction ($d=0.3$ m, $v_{max}=2$ m/s, $a_{max}=4$, $\Delta f=28\%$).
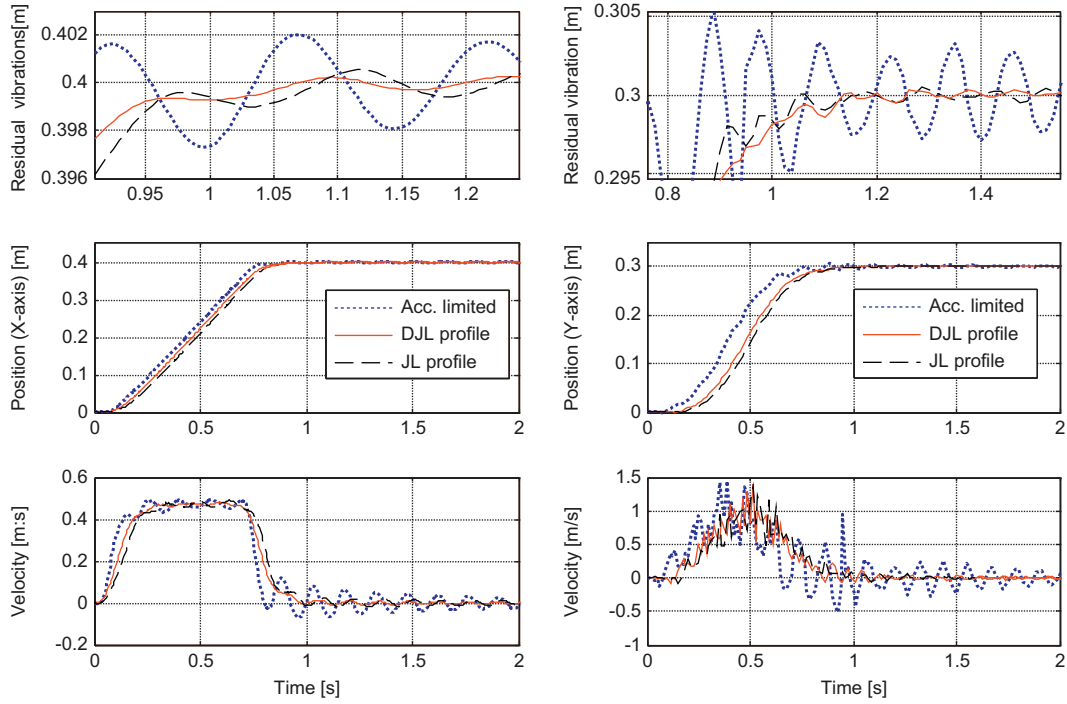
Fig. 17. Load responses measurement corresponding to the references of Fig. 16: (left) in X-direction, (right) in Y-direction.

Table 1
Characteristic measurements associated to Fig. 17.

	Acceleration limited profile		JL profile		DJL profile	
	X direction	Y direction	X direction	Y direction	X direction	Y direction
Residual vibrations [mm]	4.7 (100%)	15 (100%)	1.5 (32%)	2.2 (15%)	0.6 (12.76%)	1.2 (8%)
Rise time [s] (Theoretical)	0.947 (ref)	0.571 (ref)	1.1 (+19%)	0.704 (+23%)	1.08 (+16.5%)	0.684 (+19.8%)
Settling time [s]	2.55 (+129%)	2.4 (+112%)	1.51 (+37.7%)	1.175 (+3.2%)	1.11 (ref)	1.13 (ref)

tuned to cancel the residual vibration (jerk time is equal to the natural period of vibration at the end of the motion).

Experiments are conducted using the following set of trajectory parameters (identical for the two configurations): $d=[0,10,20,30,40,5]$ m, $v_{max}=[0.52]$ m/s, $a_{max}=4$ m/s². For each test, a comparative analysis is done for acceleration limited, JL and DJL trajectories. Fig. 16 presents two examples of reference profiles: a motion in X-direction with a constant velocity stage and a motion in Y-direction without a constant velocity stage. For these examples, the frequency shift during the motion, noted Δf, is of 20% in X-direction and 28% in Y-direction. Concerning the motion without constant velocity stage, one notes that the two intermediate jerk stages are combined with the same jerk-time, because there is no substantial variation of the period of vibration between these two stages.

Fig. 17 shows the load response measurements associated to the tests of Fig. 16 and Table 1 presents the characteristic results for these two tests. It can be observed that the amplitude of residual vibration with JL or DJL profile was significantly lower than that of acceleration-limited profile. DJL profiles verify a superior potential of vibration reduction compared to JL profile, with a reduction by 50% for the two presented tests. In the meantime, the settling time, which is a good productivity indicator, is still better for DJL profile comparatively to JL profile. If rise time is compared for the three profiles, the acceleration-limited profile gives better performances. But in the context of residual vibration reduction, the settling time for which the output has entered and remained within a specified error band

Table 2
Statistics of the DJL profile performances as compared to JL profile for the set of tests ($d=[0,10,20,30,40,5]$ m, $v_{max}=[0.52]$ m/s, $a_{max}=4$ m/s²).

	X direction	Y direction
Residual vibrations (in % as compared to JL profile)		
Mean value	−27	−19.1
Max value	−60.1	−54
Min value	0	−2
Standard deviation	18.2	10.3
Settling times (in % as compared to JL profile)		
Mean value	−11	−9.2
Max value	−37.7	−22
Min value	−4	−3
Standard deviation	13.4	7.2

(in the paper the tolerance is equal to the maximum residual vibration of DJL profile) seems more relevant.

Table 2 sums up the results for the overall experiments. Residual vibration magnitude for DJL profile is almost reduced by 23% compared to JL profile. Confronted to time-varying vibration, JL profile cannot compensate for vibration during each jerk stage. For the tests, JL profile is tuned to cancel residual vibration; hence the measured residual vibration is the result of accumulation of low-damped vibration during the first jerk stages. Moreover, the settling time (here the specified error band is chosen equal to the maximum residual vibration of DJL profile)

is reduced by 10% compared to JL profile. Now, considering the two configurations, the results are relatively close. In spite of the fact that the modal frequency variation according to Z-axis position is greater in Y-direction, the results are better for the tests in X-direction. Explanations of such difference is mainly related to the specificity of Y-axis. Y-axis is driven by a pulley-belt system for which the control structure is tuned with lower control gains compared to the two other axes. Hence, the control stiffness of Y-axis is lower and acts as an additionnal filter on the reference trajectory, which deteriorates slightly its influence on vibration.

5. Conclusions

The design and computation of near-optimal reference trajectories for CNC industrial machines is a hard challenge, which should examine the trade-off between cancellation of undesirable vibrations and rapidity. For a large class of systems, such compromise can be achieved using jerk-limited (JL) trajectory. In this paper, we focus on the extension of JL profile properties to the case of time-varying vibration problem. A dissociated jerk-limited (DJL) trajectory planning method was proposed, which consists of convolving averaging filters with adapted acceleration-limited profile. Each constant jerk stage (filter time) is tuned to reduce vibration induced at the beginning of the stage, which limit the possibility of vibration accumulation at the end of the motion. Experimental measurements, conducted on a cartesian manipulator, show that the residual vibration magnitude is reduced to less than 23% of the original level obtained with JL profile and the settling time is reduced by 10%, which prove the relevance of the proposed approach.

Appendix

The following algorithm gives the parameters of the adapted acceleration-limited profile depicted in Fig. 3, for a given sampling time T_e. According to the motion length, the maximum velocity could be reached or not. The minimum displacement allowed to reach this maximum velocity is (see Fig. 3 for notations)

$$d_{min} = \frac{2v_m{}^2 - v_0{}^2 - v_e{}^2}{2a_m} + T_F v_m$$

Case 1. If $d \geq d_{min}$. The time length of each stage will be given as

$$T_v = ceil\left(\frac{d}{v_{max}T_e} - \frac{v_{max}{}^2 - v_0{}^2}{2a_{max}v_{max}T_e} - \frac{v_{max}{}^2 - v_e{}^2}{2a_{max}v_{max}T_e}\right);$$

$$T_a = ceil\left(\frac{v_{max} - v_0}{a_{max}T_e}\right); \quad T_d = ceil\left(\frac{v_{max} - v_e}{a_{max}T_e}\right)$$

with "ceil" the function of x which returns the smallest integer greater than or equal to x.

As a consequence, the maximum values of acceleration, deceleration and velocity have to be recalculated to guarantee a perfect accuracy for the ending position and velocity (quantization errors are neglected):

$$v_{max} = \frac{2d - T_a T_e v_0 - T_d T_e v_e}{T_e(T_a + T_d + 2T_v)}; \quad a_{max} = \frac{v_{max} - v_0}{T_a T_e}; \quad d_{max} = \frac{v_{max} - v_e}{T_d T_e}$$

Case 2. $d < d_{min}$. In this case (Fig. 3b), T_v is fixed to T_F value and the reachable maximum velocity is

$$v_{max} = \frac{1}{4}(\sqrt{\delta} - 2a_{max}T_F) \text{ with } \delta = (2a_{max}T_F)^2$$
$$+ 8(v_0{}^2 + v_e{}^2 + 2a_{max}d)$$

$$T_a = ceil\left(\frac{v_{max} - v_0}{a_{max}T_e}\right) \Rightarrow a_{max} = \frac{v_{max} - v_0}{T_a T_e}$$

$$T_d = ceil\left(\frac{v_{max} - v_e}{a_{max}T_e}\right) \Rightarrow d_{max} = \frac{v_{max} - v_e}{T_d T_e}$$

References

[1] Jeon JW, Ha YY. A generalized approach for the acceleration and deceleration of industrial robots and machine tools. Proceeding of IEEE Transactions on Industrial Electronics 2000;47:133–9.
[2] Lee TS, Lin YJ. An improved sculptured part surface design with jerk continuity for a smooth machining. Proceeding of IEEE International Conference on Robotics and Automation 1998;3:2458–63.
[3] Hindle TA, Singh T. Desensitized minimum power/jerk control profiles for rest-to-rest maneuvers. In: Proceedings of the American control conference, Chigago, Illinois. 2000.
[4] Piazzi A, Visioli A. Global minimum jerk trajectory planning of robot manipulators. Proceeding of the IEEE Transactions on Industrial Electronics 2000;47:140–9.
[5] Gasparetto A, Lanzutti A, Vidoni R, Zanotto V. Experimental validation and comparative analysis of optimal time-jerk algorithms for trajectory planning. Robotics and Computer-Integrated Manufacturing 2012;28:164–81.
[6] Petrinec K, Kovacic Z. Trajectory planning algorithm based on the continuity of jerk. In: Proceedings of the 15th Mediterranean conference on control & automation, IEEE. July 27–29, Athens, Greece; 2007. p. 1-5.
[7] Gasparetto A, Zanotto V. A technique for time-jerk optimal planning of robot trajectories. Robotics and Computer-Integrated Manufacturing 2008;24(3):415–26.
[8] Béarée R, Barre PJ, Hautier JP. Vibration reduction abilities of some jerk-controlled movement laws for industrial machines, In: Proceedings of the 16th IFAC world congress, Prague, Czech Republic; July 4–8, 2005.
[9] Harris CM. Exploring smoothness and discontinuities in human motor behavior with Fourier analysis. Journal of Mathematical Biosciences 2004;188:99–116.
[10] Singh T, Singhose W. Tutorial on input shaping/time delay control of maneuvering flexible structures. In: Proceedings of the American control conference, Anchorage, AK; May 8–10, 2002.
[11] Pereira E, Trapero JR, Díaz IM, Feliu V. Adaptive input shaping for manoeuvring flexible structures using an algebraic identification technique. Automatica 2009;45(4):1046–51.
[12] Chang PH, Park HS. Time-varying input shaping technique applied to vibration reduction of an industrial robot. Control Engineering Practice 2005;13(1):121–30.
[13] Bearee R, Barre PJ, Borne P, Dumetz E. Influence of a jerk controlled movement law on the vibratory behaviour of high-dynamics systems. Journal of Intelligent and Robotic Systems 2005;42(3):275–93.
[14] Olabi A, Bearee R, Gibaru O, Damak M. Feedrate planning for machining with industrial six-axis robots. Control Engineering Practice 2010;18(5):471–82.
[15] Jeong SY, Choi YJ, Park PG, Choi SG. Jerk limited velocity profile generation for high-speed industrial robot trajectories, In: Proceedings of the 16th IFAC world congress, Prague, Czech Republic; July 4–8, 2005.
[16] Bolz RE, Tuve GL. CRC handbook of tables for applied engineering science. Boca Raton: CRC Press, Inc.; 1973 1071p.